Rev. Roum. Sci. Techn.– Électrotechn. et Énerg.
Vol. **67**, *4*, pp. 473–478, Bucarest, 2022

DOUBLE LAYER FREQUENCY SELECTIVE SURFACE WITH BROAD BANDWIDTH, HIGH SELECTIVITY, AND GOOD ANGULAR STABILITY

SUNANDA MUKHOPADHYAY[1], P SONI REDDY[1], RAHUL MONDAL[1,] PARTHA PRATIM SARKAR[1]

Keywords: Frequency selective surface; Low insertion loss; Selectivity; Angular stability; Worldwide interoperability for microwave access (Wi-MAX); C-band; Wireless local area network (WLAN).

A frequency selective surface (FSS) with low insertion loss, high selectivity, broad bandwidth, and good angular stability is proposed here. It is a patch-type FSS with two dielectric layers separated by an air gap of 1.6 mm. The bottom dielectric layer with an array of metallic patches is notified as the first FSS (FSS 1), and the top dielectric layer with an array of metallic patches is notified as the second FSS (FSS 2). In Model 1, the top surface of FSS 1 is an array of square ring-shaped metallic patches, and the bottom surface of FSS 2 is an array of square-shaped metallic patches. In Model 2, the top surface of FSS 1 is an array of square ring-shaped metallic patches, and the bottom surface of FSS 2 is an array of circular-shaped metallic patches, which are placed in a dual-layer configuration with a separation of 1.6 mm. Two reject bands are achieved as a result. Between two notch bands, a pass-band is achieved from 1.98 GHz to 5.29 GHz with good selectivity and angular stability. A notch is found at around the 3.6/4.6 GHz range, the operating band of Wi-MAX (3.3 - 3.6 GHz) and C band (3.7 GHz - 4.2 GHz). Another notch at 5.2/5.9 GHz band is achieved. The proposed FSS designs are helpful for WLAN applications.

1. INTRODUCTION

A frequency-selective surface (FSS) is any repetitive structure designed to reflect, transmit or absorb electromagnetic fields based on the frequency of the field [1, 2]. An FSS is a type of microwave filter or metal-mesh microwave filter in which the filtering is accomplished by the regular, periodic (usually metallic, but sometimes dielectric) pattern on the surface of the FSS [2]. Frequency-selective surfaces have been most commonly used in the radio frequency region of the electromagnetic spectrum and find use in applications as diverse as the aforementioned microwave oven, antenna radomes, and modern meta-materials. Many factors are involved in understanding the operation and application of frequency-selective surfaces. These include analysis techniques, operating principles, design principles, manufacturing techniques, and methods for integrating these structures into space, ground, and airborne platforms. Mainly their shape and dimension, as well as the substrate characteristic, determine the performance of an FSS [2].

In double-layer FSS, many works have been reported [3–5]. A very low loss FSS consisting of two air-spaced linear planar arrays has been reported [3]. A beam splitter achieves a low-loss pass band resonance with a sharp transmitting roll-off. A switchable slot-type frequency selective surface of a square loop is mentioned, and PIN diodes connected to a novel separated biasing circuit are presented. This structure is very thin, flexible, and sandwiched between two physically independent metallic layers to create the active filter [4]. And somewhere to improve the performance of the frequency-selective surface, especially in angular stability, the coupling of the capacitive and inductive surface is employed through a novel frequency-selective surface with high selectivity and excellent angular stability. The miniaturization of the structure unit along 0.23λ is done.

Further, to enhance the pass band of this frequency-selective surface, a multilayer frequency-selective surface is adopted to form a second-order filter [5].

A generic ACR (aperture coupled resonators), with one or both electric and magnetic coupling path, can theoretically be constructed by appropriately designing coupling apertures where an equivalent circuit model is given and analyzed using the odd and even mode method, to investigate the operating principle of ACR frequency selective surface. The model structure is a cross-dipole resonator array and one rectangular coupling aperture array in between them [6]. In another paper, a three-dimensional (3D) FSS is given, where a dual bandpass response with high selectivity and small band ratio is exhibited. The unit cell of the presented 3D structure consists of a pair of gridded double square loops (GDSLs) and a waveguide structure, where the electromagnetic coupling between the GDSLs' multiple transmission zeros and transmission poles is obtained, which result in a dual-pass band behavior with high selectivity [7]. A three-layer FSS filter is explored in a paper whose unit cell consists of identical tripole resonators located on the top and bottom layers and where rectangular coupling apertures are etched on a conducting plane between them. Multiple signal paths exist between the top and bottom resonators through these coupling apertures. Therefore, a narrow bandpass response is exhibited by this aperture-coupled resonator (ACR) structure [8].

A novel 3D FSS exhibiting band-pass filtering response with high-frequency selectivity is presented in [9]. In each unit cell, multiple resonators are constructed to provide multiple transmission zeros and poles. Furthermore, the mentioned FSS exhibited stable performance of incident angles varying from 0 to 50°, *i.e.*, it also provided angular stability. The FSS structure reported in [10] comprises two flower-shaped metallic patches on the top and bottom layers and a coupling aperture in the middle layer with a petal-shaped slot. The metallic patches are all etched on thin polyimide substrates and are supported by flexible thin Teflon substrates, which gave a flexible FSS with high out-

[1] Department of Engineering and Technological Studies, University of Kalyani, West Bengal, India
E-mail: sunanda.mukhopadhyay.bdn@gmail.com, p.sonireddy@gmail.com, rahul.mondal740@gmail.com and parthabe91@yahoo.co.in

of-suppression. A novel bandpass FSS with low pass-band insertion loss and good frequency selectivity is proposed in [11]. Each periodic cell consists of a particular cavity with a hybrid perfect electric conductor (PEC) and perfect magnetic conductor (PMC) boundary conditions, formed by four common metallic vias and complementary slots etched on both top and bottom surfaces.

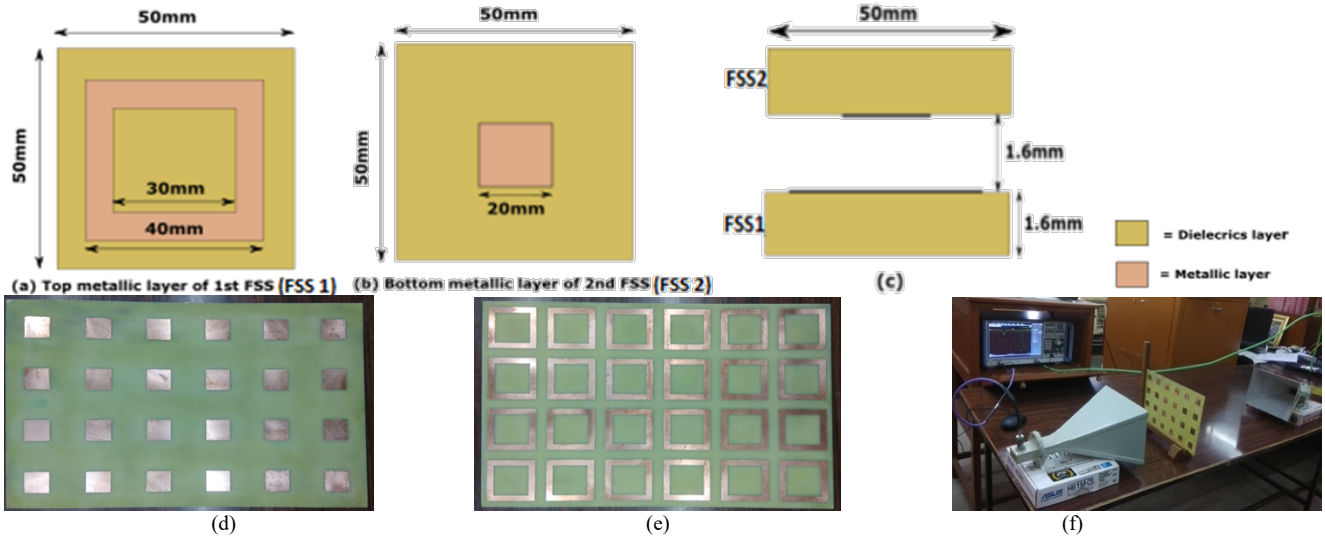

(d)

(e)

(f)

Fig. 1 – Geometry of FSS Model 1: (a) Top view of the 1st layer of FSS, (b) Bottom view of the 2nd layer of FSS, (c) Side view of double layer FSS, (d) Fabricated prototype of the FSS 1 and (e) Fabricated prototype of the FSS 2 and (f) Snapshot of the proposed FSS while testing.

In this paper, a very simple patch-type FSS is proposed. The proposed FSS designs have dual layer configurations with a separation of 1.6 mm air gap. There is no complexity in designing this model, as there are only two dielectrics and two metallic layers. Also, the shapes of the metallic patches in the two FSS models have very simple geometric shapes (square ring, square and circular type patches). It is easy to draw in software and also to simulate. For materials, copper as a metal and FR4 Epoxy as a dielectric are used, which are very cheap and available in the market. The results from those models are preferable to other works existing in literature, as, in a single FSS model, low transmission loss, high selectivity, broad pass band, and good angular stability are achieved. This can also be applicable in Wi-MAX, C-band, and WLAN purposes for having notches around 3.6/4.6 GHz and 5.2/5.9 GHz. Passing a band from 1.98 GHz to 5.29 GHz frequencies range can also be used as a bandpass filter (BPF).

2. DESIGN OF FREQUENCY SELECTIVE SURFACES

2.1 GEOMETRY OF FSS MODEL 1

The geometry details, dimensions, and fabricated prototype of the proposed FSS Model 1 are shown in Fig. 1. For achieving selectivity, angular stability, and low insertion loss of FSS, here two layers of dielectrics of FR4 Epoxy with relative permittivity of 4.4 separated by an air gap of 1.6 mm are taken. In contrast, the thickness of this dielectric slab is 1.6 mm. Here, the bottom dielectric layer is notified as the first dielectric layer, and the top dielectric layer is notified as a second dielectric layer. There is a metallic square ring patch with a dimension of 40 mm × 40 mm with 10 mm width attached on the top layer of the first dielectric, and a metallic square patch having a dimension of 20 mm × 20 mm is attached on the bottom of the second dielectric layer. For metallic patches, copper is used, and periodicity is taken as 50 mm × 50 mm.

2.2 GEOMETRY OF FSS MODEL 2

The geometry details, dimensions, and fabricated prototype of the proposed FSS Model 2 are shown in Fig. 2. Here, a patch-type FSS is designed in which two dielectric layers are separated by a 1.6 mm air gap.

A metallic square ring is patched on the top of the first dielectric layer, and a metallic circular patch is attached to the bottom of the second dielectric layer. Copper metal is used as a metallic patch and, as dielectric substrates, FR4 Epoxy with relative permittivity of 4.4 is used, whereas the thickness of FR4 Epoxy is 1.6 mm. The dimension of the top metallic patch (square ring) of the first dielectric is 40 mm × 40 mm, and its width of it is 10 mm. Where the diameter of the bottom metallic patch (circular patch) of the second dielectric substrate is 20 mm. The periodicity of this FSS is 50 mm × 50 mm.

Here, as the proposed FSS structures have dual layer configuration, an additional staggering effect is found, which increased the bandwidth of this band pass type FSS structure very efficiently between two resonances frequencies (f_r). Ansoft Designer V2 software is used to design and simulate the FSS models.

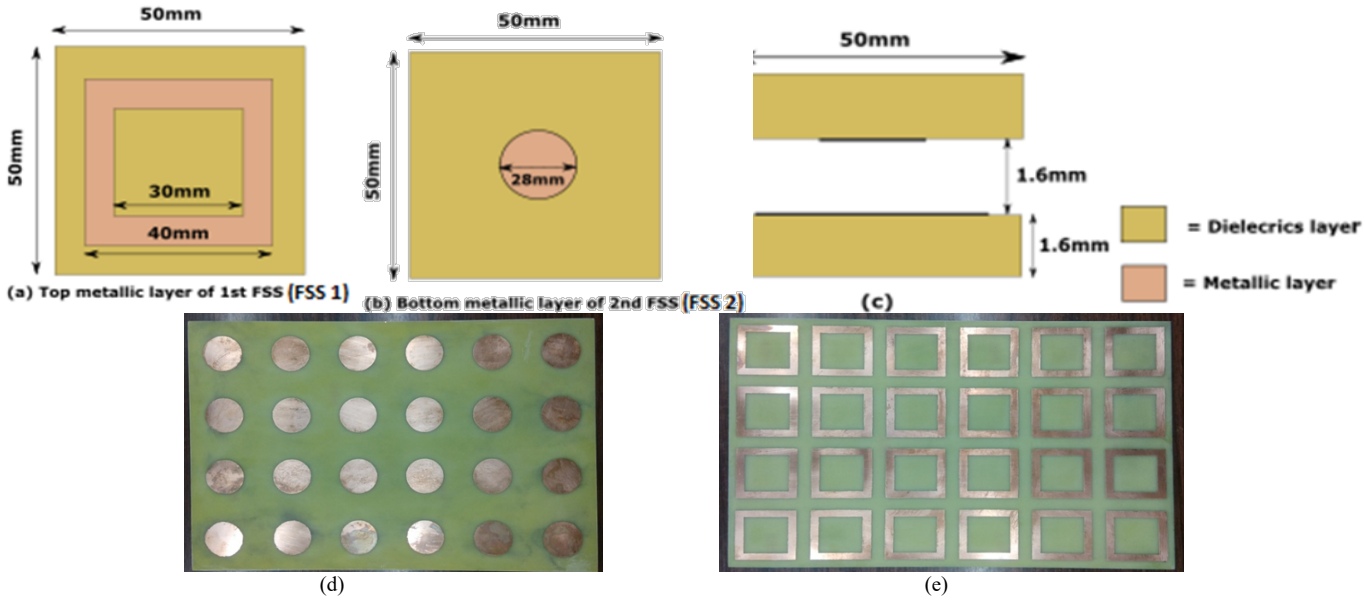

Fig. 2 – Geometry of FSS Model 2: (a) Top view of the 1st layer of FSS, (b) Bottom view of the 2nd layer of FSS, (c) Side view of double layer FSS, (d) Fabricated prototype of the FSS 1, and (e) Fabricated prototype of the FSS 2.

A patch-type FSS is designed to separate two dielectric layers by a 1.6 mm air gap. A metallic square ring is patched on the top of the first dielectric layer, and a metallic circular patch is attached to the bottom of the second dielectric layer. Copper metal is used as a metallic patch and, as dielectric substrates, FR4 Epoxy with relative permittivity of 4.4 is used, whereas the thickness of FR4 Epoxy is 1.6 mm.

3. RESULTS AND DISCUSSIONS OF FSS MODEL 1

3.1 STUDIES ON TRANSMISSION CHARACTERISTICS

For Fig. 1 (Model 1), the top metallic patch of the first FSS (FSS 1), the bottom metallic patch of the second FSS (FSS 2), and combining of them which are separated by an air gap of 1.6 mm, three transmission coefficient graphs are plotted concerning frequency in GHz (Fig. 3.a)

3.2 STUDIES ON ANGULAR STABILITY

For Fig. 1 (Model 1), the transmission coefficient graph in different incident wave angles (elevation angles variation from 0° to 30° and azimuth angles variation from 0° to 40°) are also plotted concerning frequency in GHz (Fig. 3,b and Fig. 3,c).

Here, in this proposed FSS (Fig. 1) model 1 transmission coefficient vs. Frequency graph (Fig. 3.a), of square ring metallic layer of FSS 1 and a square metallic layer of FSS 2 are plotted separately. Then combining both patches of FSS separated by a 1.6 mm air gap, their staggering graph is plotted (Table 1). In the transmission coefficient result, first, the stop resonance frequency (f_{r1}) is found at 1.88 GHz and second stop resonance frequency (f_{r2}) is at 5.69 GHz.

The lower cut-off frequency (f_L) is 2.06 GHz, and the upper cut-off frequency is (f_H) 5.29 GHz. From the simulation results, Model 1 can work at the center frequency of 2.68 GHz with a bandwidth of 3.23 GHz, whose best-case insertion loss is less than 0.29 dB. The percentage of the bandwidth of this Model 1 is 120.6 %.

In addition, the band edge of the proposed model 1 is reasonably sharp. Here, good selectivity is also achieved (Table 2). The uphill slope is 155.67 dB/GHz, and the downhill slope is 68.64 dB/GHz. Comparing this result with the designed results in [5], this model 1 has a better passband performance. This Model 1 is also angularly stable (Fig. 3.b and Fig. 3.c) in both variations of elevation and azimuth angles. Model 1 is angularly stable concerning elevation angle (θ) from 0° to 30° and concerning azimuth angle (φ) from 0° to 40° (Tables 3 and 4).

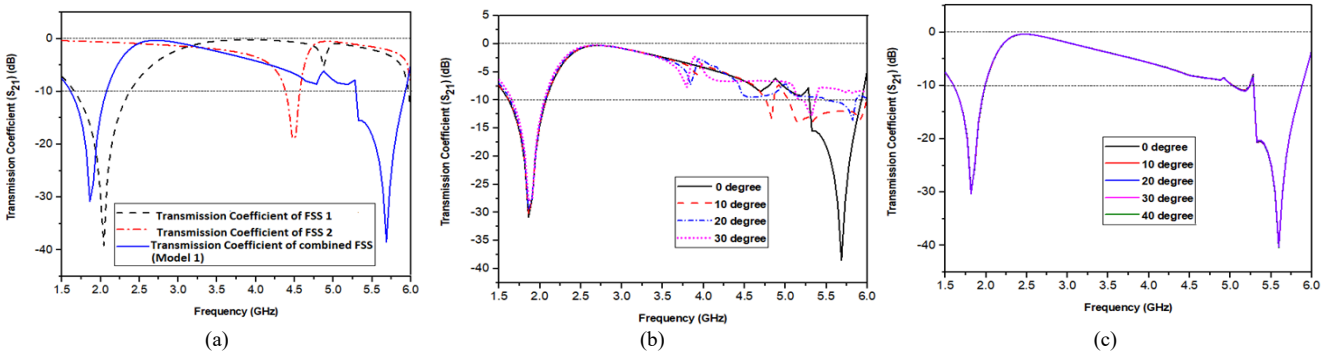

Fig. 3 – (a) Simulated result of transmission coefficient graphs of square ring (FSS 1), square (FSS 2) and combining of both FSS1 and FSS2 figures, (b) Simulated result of transmission coefficient graph of Model 1 FSS under different incident wave angles of theta (elevation angle variation from 0 to 30 degree), (c) Simulated result of transmission coefficient graph of Model 1 FSS under different incident wave angles of phi (azimuth angle variation from 0 to 40 degree).

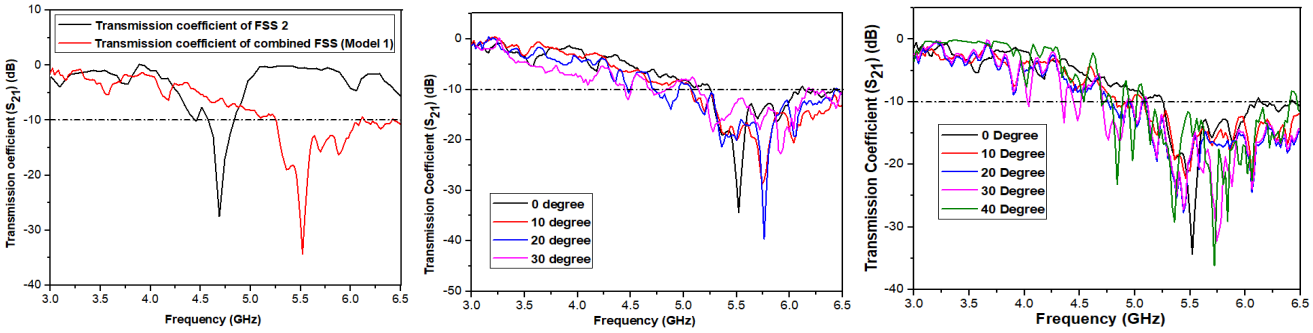

(a) (b) (c)

Fig. 4 – (a) Measured result of transmission coefficient graphs of square (FSS 2) and combining of both FSS 1 and FSS 2 figures, (b) Measured result of transmission coefficient graph of Model 1 FSS under different incident wave angles of theta (elevation angle variation from 0 to 30 degree), (c) Measured result of transmission coefficient graph of Model 1 FSS under different incident wave angles of phi (azimuth angle variation from 0 to 40 degree).

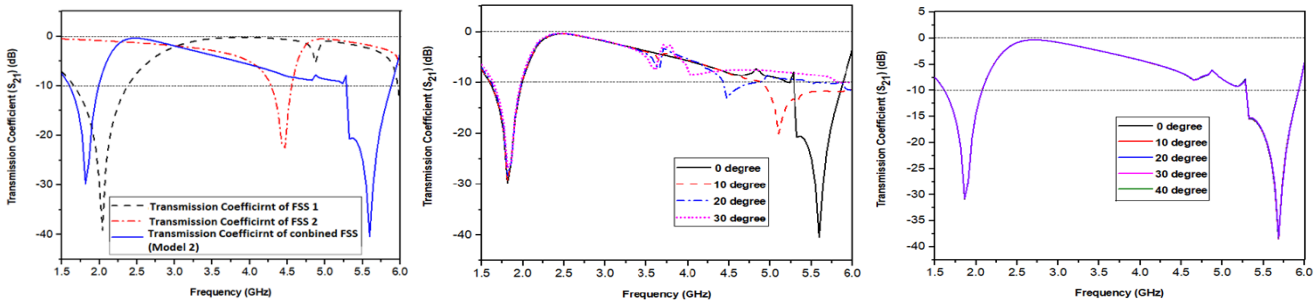

(a) (b) (c)

Fig. 5 – (a) Simulated result of transmission coefficient graphs of square ring (FSS 1), circle (FSS 2) and combining of both FSS 1 and FSS 2 figures, (b) Simulated result of transmission coefficient graph of Model 2 FSS under different incident wave angles of theta (elevation angle variation from 0 to 30 degree), (c) Simulated result of transmission coefficient graph of Model 2 FSS under different incident wave angles of phi (azimuth angle variation from 0 to 40 degree).

So, high bandwidth and a bandpass filter (BPF) with a high transmission coefficient value (0.29 dB) at 2.68 GHz resonance frequency and high selectivity are achieved here. The measured transmission characteristics and angular stability plots of the proposed FSS Model 1 are given in Fig. 4. It is observed that the measured results follow the simulated results.**4.** Results and Discussions of FSS Model 1

4.1 STUDIES ON TRANSMISSION CHARACTERISTICS

For Fig. 2 (Model 2), the top metallic patch of the first FSS (FSS 1), the bottom metallic patch of the second FSS (FSS 2), and combining of them which are separated by an air gap of 1.6 mm, three transmission coefficient graphs are plotted concerning frequency (Fig. 5.a).

4.2 STUDIES ON ANGULAR STABILITY

For Fig. 2 (Model 2), the transmission coefficient graph in different incident wave angles (elevation angles variation from 0° to 30° and azimuth angles variation from 0° to 40°) is also plotted concerning frequency (Fig. 5.b and Fig. 5.c). Here, in this proposed FSS (Fig. 2), Model 2 at first transmission coefficient vs. frequency graph (Fig. 5.a) of square ring shape metallic patch of FSS 1 and circular shape metallic patch of FSS 2 are plotted individually. Both patches, FSS 1 and FSS 2, are combined, separated by an air gap of 1.6 mm.

Their transmission coefficient vs. frequency graph is plotted to study the staggering effect (Table 1). In this transmission coefficient result, the first stop resonance frequency (f_{r1}) is found at 1.81 GHz, and the second stop resonance frequency (f_{r2}) is at 5.60 GHz. The lower cut-off frequency (f_L) is 1.99 GHz, and the upper cut-off frequency is (f_H) 5.29 GHz. From the simulation results, the FSS can work at the center frequency of 2.44 GHz with a bandwidth of 3.30 GHz, whose insertion loss is less than 0.33 dB. So, the percentage of bandwidth achieved is 135.3%. Here, very good selectivity is also achieved, as shown in Table 2. The uphill slope is 116.50 dB/GHz, and the downhill slope is 98.13 dB/GHz.

Table 1

Stop band frequencies comparison between two FSS models at 0° incident angle

Type of FSS	FSS Layers	1st stop freq. (GHz)	2nd stop freq. (GHz)
Model 1	FSS 1	2.04	-
	FSS 2	-	4.48
	Staggering (FSS 1 + FSS 2)	1.88	5.69
Model 2	FSS 1	2.04	-
	FSS 2	-	4.50
	Staggering (FSS 1 + FSS 2)	1.81	5.60

This Model 2 is also angularly stable in the variation of elevation and azimuth angles (Fig. 5.b and Fig. 5.c). Model 2 is angularly stable concerning elevation angle (θ) from 0° to 30° and for azimuth angle (φ) from 0° to 60° (Table 3 and Table 4). So, this Model 2 frequency selective surface is more selective here than the previous one. Not only that but here, very good bandwidth is also achieved. So, both the models exhibit very good angular stability in both look angles (θ and φ), where in azimuth angle variation from 0° to 40° there is no change in the value of bandwidth, transmission coefficient value, up and downhill slopes, *etc.* (Table 3 and Table 4). This is perfectly the same in all azimuth angles variation. The measured transmission characteristics and angular stability plots of the proposed FSS Model 2 are given in Fig. 6. It is observed that the measured results follow the simulated results.

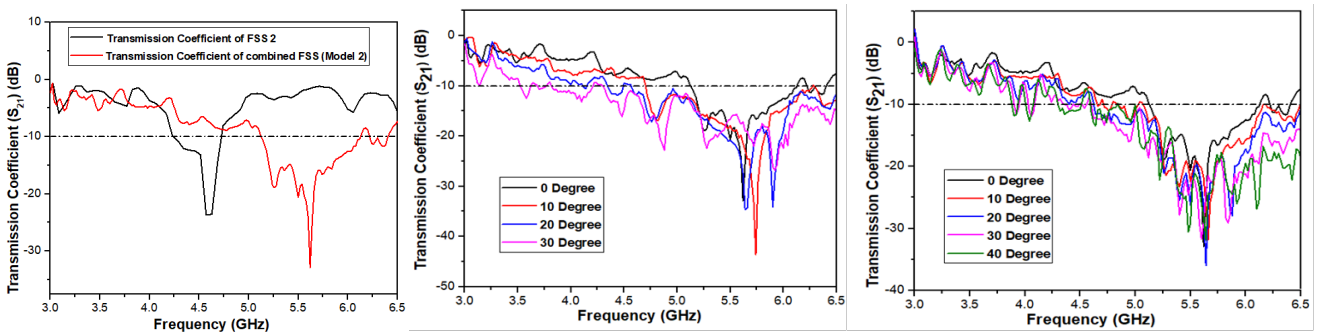

(a) (b) (c)

Fig. 6 – Measured result of transmission coefficient graphs of, square (FSS 2) and combining of both FSS 1 and FSS 2 figures, (b) Measured result of transmission coefficient graph of Model 2 FSS under different incident wave angles of theta (elevation angle variation from 0 to 30 degree), (c) Measured result of transmission coefficient graph of Model 1 FSS under different incident wave angles of phi (azimuth angle variation from 0 to 40 degree).

Table 2

Bandwidth and selectivity comparison between two FSS models at 0° incident angle

Type of FSS	Pass Band				Uphill slope dB/GHz	Downhill slope dB/GHz
	f_L GHz	f_H GHz	BW GHz	% of BW		
Model 1	2.06	5.29	3.23	120.6	155.67	68.64
Model 2	1.99	5.29	3.30	135.3	116.50	98.13

Table 3

Higher (f_H) and lower (f_L) cut-off frequencies comparison between two FSS models with a variation of elevation angle (θ) from 0° to 30°

Type of FSS	f_L (GHz)				f_H (GHz)			
	0°	10°	20°	30°	0°	10°	20°	30°
Model 1	2.06	2.07	2.06	2.08	5.29	4.76	5.49	5.24
Model 2	1.99	1.99	1.98	1.98	5.29	4.68	4.43	5.75

Table 4

Bandwidth (BW) and % of bandwidth comparison between two FSS models with a variation of elevation angle (θ) from 0° to 30°

Type of FSS	BW (GHz)				% of BW			
	0°	10°	20°	30°	0°	10°	20°	30°
Model 1	3.23	2.69	3.43	3.16	120.6	100	128.5	118.8
Model 2	3.30	2.69	2.45	3.77	135.3	109	100.5	154.6

5. PERFORMANCE COMPARISON

The performance of the proposed FSS models (Model 1 and Model 2) has been compared with some of the existing multi-layer FSS designs in the literature, and the results are shown in Table 5.

Compared to the existing designs [4–6, 9, 10], the proposed FSS models provide higher selectivity on either side of the operating band. The total height of the proposed FSS models is also lower than the compared FSS structures. The proposed FSS models also have good angular stability for $\phi = 0°–40°$ and $\theta = 0°–30°$.

6. CONCLUSION

This paper achieves an FSS structure with high selectivity and broad bandwidth. This proposed frequency-selective surface is a patch-type FSS. Here, two stop bands are found, and a pass-band is achieved between them. The bandwidth of this proposed FSS is 3.3 GHz, and the percentage of bandwidth is 135.3 %.

To improve the angular stability, the coupling of the capacitive surface and the inductive surface is employed, which provides good angular stability for both Model 1 and Model 2 from 0° to 30° in elevation angles and from 0° to 40° in azimuth angles. This FSS structure can be used in high data transmission with low transmission losses, high selectivity, and excellent angular stability.

For having notch bands at around 3.6/4.6 GHz, the proposed FSS models are useable in WiMAX (3.3-3.6 GHz) and C-band (3.7-4.2 GHz) applications. Another notch band at 5.2/5.9 GHz band is achieved, which is useable in WLAN applications.

The proposed FSS models have a pass-band from 1.98 GHz to 5.29 GHz frequencies range thus, it can also be used as a bandpass filter (BPF).

Table 5

Performance comparison of the proposed FSS designs with the existing FSS designs in the literature

References	No. of FSS Layers	Operating Bandwidth	Selectivity	Angular Stability	Height (mm)	Applications
[4]	Dual Layer	1.5-3.75 GHz	Low Uphill slope = 0.07 dB/GHz Downhill slope = 16.15 dB/GHz	NA	20	Wall of a building, Bluetooth
[5]	Four Layers	27-31 GHz	Low Uphill slope = 7.5 dB/GHz Downhill slope = 35 dB/GHz	Good $\phi = 0°$ to $60°$ $\theta = \pm 45°$	NA	5G communication, Radome
[6]	Three Layers	Narrow Band at 60 GHz	Low Uphill slope = 7.5 dB/GHz Downhill slope = 3.07 dB/GHz	Low No ϕ variation $\theta = 0°$ to $40°$	NA	Millimeter wave, Terahertz frequencies

[9]	Three Layers	29-30 GHz	Low Uphill slope = 13.33 dB/GHz Downhill slope = 13.33 dB/GHz	Good ϕ = 0° to 50° θ = 0° to 50°	5.11	Communications satellite, Ka band
[10]	Three Layers	14.6- 19.8 GHz	Low Uphill slope = 2 dB/GHz Downhill slope = 23.5 dB/GHz	Good No ϕ variation θ = 0° to 40°	NA	K band
Proposed FSS Model 1	Dual Layer	2.04-5.29 GHz	High on both the sides of the desired band Uphill slope = 155.67 dB/GHz Downhill slope = 68.64 dB/GHz	Good for both θ and φ angles ϕ = 0° to 40° θ = 0° to 30°	4.8	WiMAX, WLAN, and C band
Proposed FSS Model 2	Dual Layer	1.98 to 5.29 GHz	High on both the sides of the desired band Uphill slope = 116.50 dB/GHz Downhill slope = 98.13 dB/GHz	Good for both θ and φ angles ϕ = 0° to 40° θ = 0° to 30°	4.8	WiMAX, WLAN, and C band

Received on 31 January 2022

REFERENCES

1. T.K. Wu, *Assini frequency Selective surface development*, J. Electromagnet waves Applications, 8, 12, pp. 1547-1561, Dec.1994.
2. B.A. Munk, *Frequency selective surfaces: theory and design*, John Wiley & Sons, Chapter 5, pp. 28-58 (2005).
3. R. Cahill, J.C.Vardaxoglou, M. Jayawardene, *Two-layer mm-wave FSS of linear slot elements with low insertion loss*, IEEE Proc.-iMicrowave. Antennas Propagation, **148**, *6*, pp. 2179-1074, (2001).
4. B. Sanz-Izquierdo, E.A. Parker, J.C. Bachelor, *Switchable frequency selective slot arrays*, IEEE transactions on antennas and propagation, **597**, pp. 2728-2731 (2011).
5. T.W. Li, D. Li, E.P. Li, *A novel fss structure with high selectivity and excellent angular stability for 5G communication radome*, 2017 10th Global Symposium on Millimeter-Waves, pp. 50-52 (2017).
6. D.S. Wang, P. Zhao, *Design and analysis of a high-selectivity frequency-selective surface at 60 GHz*", IEEE Trans. on Microwave Theory and Techniques, **64**, *6*, pp. 1694-1703 (2016).
7. Z. Yu, X. Yang, J. Zhu, C. Wang, Y. Shi, W. Tang, *Dual-band three-dimensional FSS with high selectivity and small band ratio*, Electronics Letters, **55**, *14*, pp. 798–799 (2019).
8. D.S. Wang, B.J. Chen, C.H. Chan, *High-selectivity band pass frequency-selective surface in terahertz band*", IEEE Transactions on Terahertz Science and Technology, **6**, *2*, pp. 284-291 (20160.
9. K. Tao, B. Li, Y. Tang, M. Zhan, Y. Bo, *Analysis and implementation of 3D bandpass frequency selective structure with high-frequency selectivity*, Electronics Letters, **53**, *5*, pp. 324–326 (2017).
10. H.L. Li, B. Wu, Y.T. Zhao, T. Su, *design of flexible bandpass frequency selective surface with high out-of-band suppression*", 2018 IEEE Asia-Pacific Conference on Antennas and Propagation (APCAP), pp. 281-282 (2018).
11. G.L. Dai, W. In, X C. Wei, E.P. Li, *A novel FSS based on hybrid boundary condition cavity*", 2012 Asia-Pacific Symposium on Electromagnetic Compatibility, pp. 473-476 (2012).